Evacuated Waveguide Filter for Suppressing Spurious Transmission from High-Power *S*-Band Radar*

H. A. WHEELER† AND H. L. BACHMAN†

Summary—A one-megawatt magnetron, used in a search radar, tunes over the *S* band of 3.1 to 3.5 kmc, and simultaneously causes interference in the band of 3.7 to 4.0 kmc by occasional oscillation in spurious modes. For insertion in the antenna line of this radar, a band-pass filter has been designed to provide over 120 db attenuation in the interference band. It is a wave filter with *M*-derived terminations for impedance matching and with three sections including traps resonant in the stop band, for high attenuation, all made of nine resonant irises spaced ¼ wavelength in a waveguide. Each filter is sealed by pressure windows and evacuated to handle the high-power pulses. Two such filters are connected in parallel between 3-db directional couplers to make a nonreflecting assembly.

Introduction

THE FILTER to be described has been developed to meet some unusual requirements, by means of an advanced design in waveguide, together with special provisions to handle high-power pulses. The M-33 Fire Control System contains a search radar which was found to cause interference with microwave relay links operating in a slightly higher frequency band. It was determined that the *S*-band magnetron, which is intended to oscillate in the 8-mode (or pi-mode), transmits also some spurious high-power pulses on a higher frequency corresponding to the 7-mode. Therefore, a filter was needed to suppress the spurious pulses while passing the normal pulses.

The most severe requirement of this filter is the transmission of high-power (one-megawatt) pulses through the resonant circuits that form the filter. This dictated the use of a waveguide structure with special provisions for handling the high electric gradients (such as a vacuum). The required amount of attenuation is obtained in the waveguide environment by structural elements simulating a carefully computed lumped circuit. The further requirement of avoiding substantial reflection is met by assembling a pair of such filters between two directional-coupler hybrid junctions. This arrangement is patterned after the well-known balanced duplexer, which behaves as a nonreflecting filter below the power level of breakdown within the filter structure. Here the interior will be evacuated to an unusually high degree to preclude breakdown in the dielectric space.

This paper presents a general description of the nonreflecting filter assembly, a complete description of the wave filter with design formulas, a procedure for realizing such a filter in a waveguide structure, and the results obtained in a practical design. A particular feature is the evaluation of the reactance arms of the filter in a form normalized for resonators in a waveguide, and suited for testing the realization of these arms.

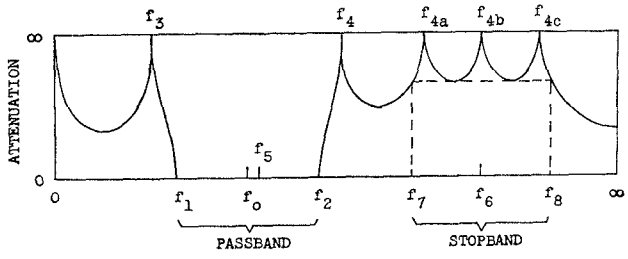

Fig. 1—Attenuation over frequency range.

Fig. 1 is a frequency diagram showing the basis for specifying and realizing the required attenuation. The principal frequency bands are the pass band in which no attenuation is desired and the stop band in which high attenuation is desired.

The frequency band of the radar is 3.1–3.5 kmc. A nominal pass band was chosen, 1.25 times as wide, between cutoff frequencies of 3.05 and 3.55 kmc. The interference band or stop band was designated as 3.7–4.0 kmc which covers the overlap between the 7-mode band (3.50–3.95 approx) and the TD-2 relay band (3.70–4.20). The objective of high attenuation over the interference band was satisfied with a computed attenuation greater than 120 db.

After a list of symbols, there will be a general description of the complete filter arrangement and its capabilities, followed by the formulas for the filter sections and the computations for the present purpose.

Symbols

R = mid-series image resistance at midband
G = mid-shunt image conductance at midband
jG = impedance inverter based on G
L = inductance in arm of half-section
C = capacitance in arm of half-section
C_0, L_0 = elements of series arm of constant-K half-section
X = reactance of series arm of half-section
B = susceptance of shunt arm of half-section
$b = B/G$ = susceptance ratio (normalized susceptance)

* Manuscript received by the PGMTT, May 14, 1958; revised manuscript received, July 28, 1958. More comprehensive formulas and rules are available from the authors on request.
† Wheeler Labs., Great Neck, N. Y.

av $|b|$ = average magnitude of b at f_1 and f_2
$Q = \omega L/R$ of series resonance
$Q = \omega C/G$ of shunt resonance
$\omega = 2\pi f$ = radian frequency
f = cycle frequency
f_c = cutoff frequency of low-pass analog
f_∞ = trap frequency of low-pass analog
$f_0 = \sqrt{f_1 f_2}$ = midfrequency of pass band
$f_8 = \sqrt{f_7 f_8}$ = midfrequency of stop band
λ_0 = wavelength in waveguide at f_0
m = parameter of M-derived half-section (VI type)
m_5 = parameter of derived half-section (V type)
α = attenuation of half-section (on image basis) (napiers)
$\exp -\alpha$ = response ratio of symmetric section = output/input ratio of voltage or current
sub-0 = midband
sub-1, 2 = cutoff frequency at edge of nominal pass band
sub-3, 4 = trap frequency (VI type)
sub-7, 8 = edge of stop band (V type)
sub-4, 4*a*, 4*b*, 4*c* = trap frequency (V type)
sub-5, *a*, *b*, *c* = series arm of derived half-section (V type)
sub-*oa*, *ab*, *bc*, *oc* = full-shunt arm made of the two mid-shunt arms at junction of two different half-sections
Type IV = constant-K band-pass filter (no trap frequencies)
Type VI = M-derived band-pass filter (symmetrical trap frequencies)
Type V = band-pass filter with single trap frequency above the band.

The Nonreflecting Assembly

A wave filter attenuates by reflection. It happens that a magnetron will emit even more spurious pulses if the load presents too much reflection in the frequency range of these pulses. Therefore, the solution of the present problem requires a nonreflecting filter assembly. This result is achieved by using a matched pair of wave filters in a certain environment based on well-known principles.

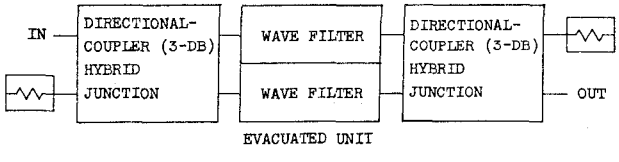

Fig. 2—Diagram of nonreflecting filter assembly.

Fig. 2 shows the essentials of the nonreflecting filter assembly, patterned after the balanced duplexer. Two identical wave filters are connected between input and output terminal junctions, each being a four-port with one of its ports connected to a dummy load.

Each terminal junction is essentially a hybrid junction supplemented by a phase difference of 90° between one pair of ports and the other pair. These properties are combined in the well-known 3-db directional coupler, so this component is utilized.

The resulting assembly retains the transmission and attenuation properties of the wave filters because the pair of filters are essentially connected in parallel between the indicated input and output ports. However, the reflections from the two filters at either end are canceled out, as seen from the input or output port, and the reflected power is diverted to the dummy load at the corresponding end. In this way, the complete assembly becomes a nonreflecting filter.

The entire nonreflecting filter in its operating environment is shown in a more recent presentation by R. D. Campbell, dealing with the operational situation that requires this filter [19].

The Wave Filter

The wave filter is essentially a band-pass filter designed on the basis of image parameters. It comprises a number of sections chosen to meet the requirements with economy in the number of parts. It is embodied in a waveguide structure by means of several specialized irises with proper spacing.

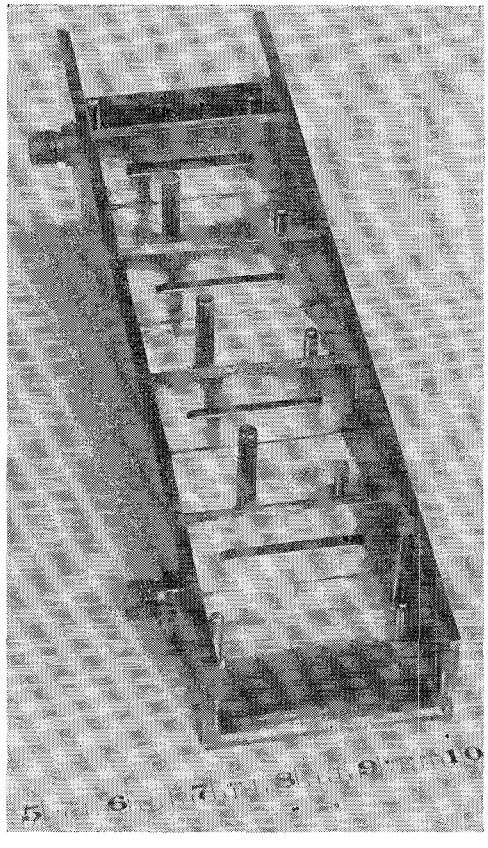

Fig. 3—Photo of wave filter (top removed).

Fig. 3 shows the type of construction used for each wave filter. As will be explained further on, the filter is to be evacuated to prevent breakdown in the dielectric space, so it is constructed in a waveguide section suitable for sealing with pressure windows at the ends. The

internal pieces comprise the irises which make the filter. (This particular structure is a preliminary model which differs from the final design in minor details, especially in having thicker internal partitions.)

Fig. 4 shows the equivalent lumped networks which form the basis for the waveguide structure. In a waveguide, shunt arms are easy to make because they can be inserted while the walls remain intact, while series arms are very difficult, requiring breaks in the walls and the addition of external parts. Fig. 4(a) shows how the complete filter is made of shunt arms in a waveguide, while 4(b) shows the equivalent ladder network of shunt and series arms.

The waveguide form in Fig. 4(a) obtains the effect of shunt and series arms by using shunt arms spaced $\frac{1}{4}$ wavelength in the guide. This is a well-known principle, exemplified in evacuated TR tubes that formed the background of the present development.

Each of the arms of the filter is resonant in the pass band. Alternate arms are also antiresonant at one or two trap frequencies just outside the pass band. In the end arms, the trap frequencies are used for image-impedance matching over the useful part of the pass band. In the intermediate arms, the trap frequencies are used for high attenuation in the stop band.

Next there will be presented in some detail the design of the wave filter.

Image-Parameter Design

The time-honored image-parameter viewpoint of Campbell and Zobel, as summarized by Shea, offers the only practical method for designing a filter of this degree of complexity [1, 2]. There are 25 lumped constants to be computed. There is no symmetry about the pass band, so we cannot use a low-pass analog to reduce to one-half the number of constants to be evaluated. The pass band and stop band are of such width and proximity that no simplifying assumptions are valid. The large number of elements makes it necessary to compute each one within close tolerances. The method of image parameters enables straightforward computations with reasonable simplicity.

Fig. 4 shows the complete filter arrangement to be computed, while Fig. 1 shows the attenuation pattern to be obtained. The kind of sections and the number of sections have been chosen to meet the requirements of this development, considering various factors that will be mentioned.

The filter is shown as a succession of shunt arms (9 as required for 8 contiguous half-sections) separated by quarter-wave sections or inverters. This is common practice in waveguides. Two types of sections are used. Most of the attenuation is provided by 3 sections of V type, a double-tuned section with a trap frequency above the pass band. At each end, impedance matching is provided by a half-section of the well-known M-derived VI type [1, 2]. These type designations are the customary ones based on the number of elements in one half-section (5 and 6 in these cases).

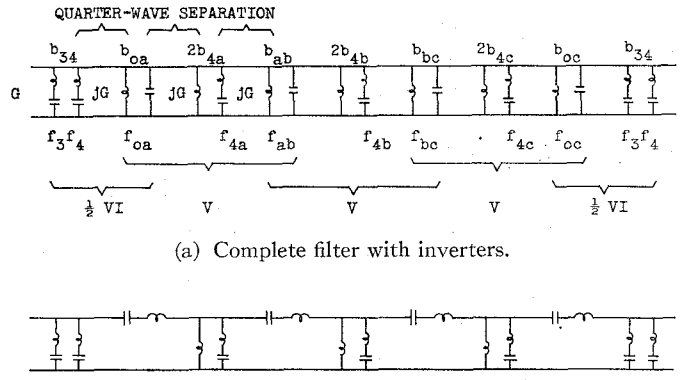

(a) Complete filter with inverters.

(b) Equivalent filter in ladder form.

Fig. 4—Complete band-pass wave filter of eight half-sections.

The attenuation pattern shows the nominal pass band (between cutoff frequencies) and the basis for defining the stop band (including 3 trap frequencies). In the present case, these bands are specified as mentioned above and in the example computed below. The two trap frequencies just above and below the pass band are determined by the impedance-matching requirement in the end half-sections.

The immediate purpose is to give the formulas for computing the lumped reactance arms in this filter. They will be evaluated in terms of shunt susceptance, this being suitable for realization and testing in shunt arms in a waveguide. This is the most direct way of specifying the required properties of the reactance arms which make up the filter.

Referring to the problem of voltage breakdown, the voltage at all the shunt arms, except the end arms, increases near the cutoff frequencies. This is a result of the increasing image resistance at these junctions. By using only 0.8 of the nominal pass band, the ratio of excess voltage, relative to midband, is held down to about 1.3, for the same pulse power.

In the pass band, the principal problem is impedance matching, which means avoiding reflections in the "confluent" wave filter. Dissipative attenuation is less important, except near the cutoff frequencies. In general, it is proportional to the phase slope and to the average dissipation factor of all the reactance elements. These factors combine to make such attenuation negligible over the utilized fraction of the pass band, so it is ignored in the design procedure.

The VI type is selected for the end half-sections because it is the simplest that can give, over 0.8 of the pass band, an image resistance that approximately matches a constant resistance. In this design, the image resistance at the ends of the filter is theoretically between the midband value and another value lower by 0.04 of the midband value. In order to obtain this property, the trap frequencies must be separated by 1.25 times the nominal bandwidth, so their values cannot be chosen for greatest benefit in attenuation.

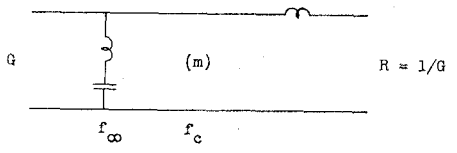

(a) Low-pass M-derived half-section (for reference).

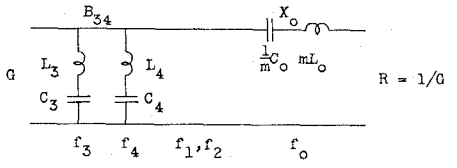

(b) VI-type M-derived half-section.

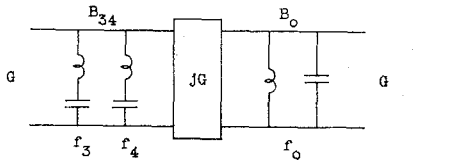

(c) VI-type half-section with inverter.

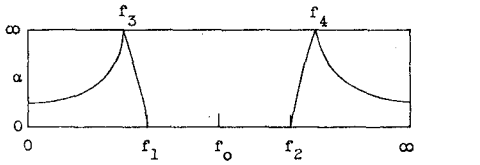

(d) Attenuation over frequency range.

Fig. 5—VI-type filter half-section.

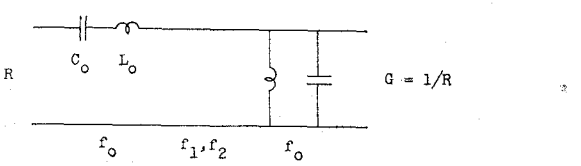

(a) IV-type constant-R half-section (for reference).

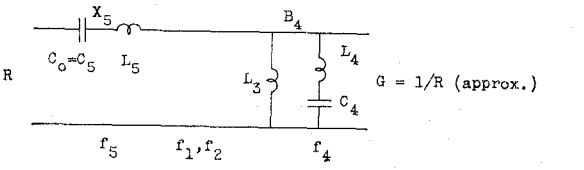

(b) V-type half-section.

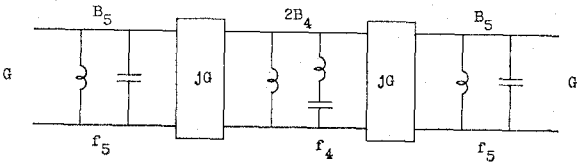

(c) V-type whole section with inverters.

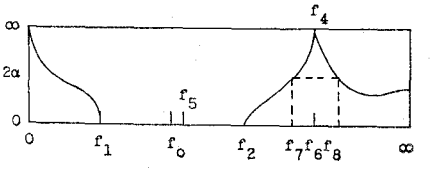

(d) Attenuation over frequency range.

Fig. 6—V-type filter section.

The V type is chosen for the repeating whole sections because it is the type of section that gives the greatest attenuation over a stop band just above the pass band. It was estimated that three such sections would give more than sufficient attenuation.

The actual attenuation or insertion loss outside the pass band is that obtained when the filter is connected between generator and load of equal values of constant resistance. This condition is approximated in practice. The actual attenuation always exceeds the image attenuation, so the latter is safely assumed as a basis for estimating the required number of sections

The inverter or quarter-wave section is a part of this design [4], [6], [7], [9], [10]. It enables a ladder network of series and shunt arms to be simulated by a sequence of shunt arms, the kind best suited for a waveguide structure. Theoretically, the inverter is a section of waveguide having a length of one-quarter wave at all frequencies. It is so called because any impedance, seen through the inverter, appears to have its value inverted about the wave resistance of the inverter. Since G is the wave conductance at midband, the symbol for the inverter is jG; this is chosen because the equivalent pi or T network has three arms of values $\pm jG$. In practice, the effective length of the quarter-wave section varies somewhat over the pass band, and these variations are taken into account in the design of the adjacent shunt arms. There is one inverter per half-section; this determines the total length in waveguide.

Having given a general description of the filter, there follows a more specific description of each of the two types of sections (Shea, [1], [2]).

Fig. 5 shows the VI-type half-section. Since its properties have ratio symmetry about the midfrequency (meaning, the same properties at equal frequency ratios above and below the midfrequency), this type has a low-pass analog [Fig. 5(a)] which is a helpful reference in formulating the band-pass filter. The low-pass cutoff frequency (f_c) is half the bandwidth of the band-pass filter (f_2-f_1). The low-pass trap frequency (f_∞) is similarly related to the band-pass trap frequencies (f_3, f_4).

The band-pass half-section [Fig. 5(b)] is shown in conventional ladder form. The series arm is evaluated in terms of the corresponding constant-K (IV type) series arm (C_0, L_0) and the constant (m) of this M-derived type. The inverter form [Fig. 5(c)] has two shunt arms (instead of one shunt and one series) separated by the inverter (jG). Each shunt arm contains the indicated susceptance (B_{34}, B_0). The attenuation diagram [Fig. 5(d)] shows the variation of the attenuation (α) outside the pass band.

Fig. 6 shows the V-type section. Since its properties do not have symmetry about the pass band, there is no low-pass analog. A helpful reference is the IV-type band-pass half-section [Fig. 6(a)]. Its series and shunt arms are resonant at the midfrequency (f_0). The V-type half-section [Fig. 6(b)] has a series arm resonant at a frequency (f_5) within the pass band but above midband. The shunt arm as a whole is resonant at the same fre-

TABLE I
FORMULAS FOR VI TYPE

$$m = 0.6 \tag{1}$$

$$f_c = \frac{f_2 - f_1}{2} \tag{2}$$

$$f_\infty = \frac{f_4 - f_3}{2} = \frac{f_c}{\sqrt{1 - m^2}} = 1.25 f_c \tag{3}$$

$$f_0 = \sqrt{f_1 f_2} = \sqrt{f_3 f_4} \tag{4}$$

$$f_1, f_3 = \sqrt{f_0^2 + f_\infty^2} \pm f_\infty \tag{5}$$

$$Q_0 = \frac{m L_0 \omega_0}{R} = \frac{m f_0}{f_2 - f_1}. \tag{6}$$

At f_1 and f_2:

$$|b_0|_1 = |b_0|_2 = m = 3/5 \tag{7}$$

$$|b_{34}|_1 = |b_{34}|_2 = 1/m = 5/3. \tag{8}$$

At $f = 0$ or ∞:

$$\sinh \alpha = \frac{m}{\sqrt{1 - m^2}} = 3/4; \alpha = 0.693 = 6.02 \text{ db}. \tag{9}$$

Note: 1 napier = 8.686 db.
Note: Over 4/5 of nominal pass band, this value of m holds the reflection coefficient less than 0.020 at each M-derived termination; for two terminations, SWR < 0.7 db.

TABLE II
FORMULAS FOR V TYPE

For $\cosh \alpha_7 = \sinh \alpha_8$;

$\alpha_7 \doteq \alpha_8$ if $\exp -2\alpha_7 \ll 1$:

$$f_4^2 = f_7^2 + \frac{f_8^2 - f_7^2}{1 + \frac{f_7^2}{f_8^2}\left(\frac{f_8^2 - f_5^2}{f_7^2 - f_5^2}\right)^2}. \tag{10}$$

Before f_5 is known, substitute f_0 as approximation in preceding formula

$$m_5 = \frac{1 - \left(\frac{f_2 - f_1}{\sqrt{f_4^2 - f_1^2} + \sqrt{f_4^2 - f_2^2}}\right)^2}{1 + \left(\frac{f_2 - f_1}{\sqrt{f_4^2 - f_1^2} + \sqrt{f_4^2 - f_2^2}}\right)^2} \tag{11}$$

$$f_5 = f_0/\sqrt{m_5} = \sqrt{f_1 f_2/m_5} \tag{12}$$

$$f_6 = \sqrt{f_7 f_8} \tag{13}$$

$$Q_5 = \frac{L_5 \omega_5}{R} = \sqrt{m_5}\,\frac{f_0}{f_2 - f_1} \tag{14}$$

At f_1: $|b_5|_1 = |1/b_4|_1 = 1 + (1 - m_5)\dfrac{f_1}{f_2 - f_1}$ (15)

At f_2: $|b_5|_2 = |1/b_4|_2 = 1 - (1 - m_5)\dfrac{f_2}{f_2 - f_1}$ (16)

$$\text{av}\,|b_5| = \text{av}\,|1/b_4| = \frac{1 + m_5}{2} \tag{17}$$

$$\cosh \alpha_7 = \frac{f_2(f_7^2 - f_5^2)}{f_7(f_2^2 - f_5^2)}\sqrt{\frac{f_4^2 - f_2^2}{f_4^2 - f_7^2}} \tag{18}$$

$$\sinh \alpha_8 = \frac{f_2(f_8^2 - f_5^2)}{f_8(f_2^2 - f_5^2)}\sqrt{\frac{f_4^2 - f_2^2}{f_8^2 - f_4^2}}. \tag{19}$$

At $f = \infty$: $\sinh \alpha = \dfrac{f_2\sqrt{f_4^2 - f_5^2}}{f_2^2 - f_5^2}$. (20)

If $f_4/f_5 < \sqrt{2}$, there is a minimum attenuation at

$$f = \frac{f_4}{\sqrt{2 - (f_4/f_5)^2}}: \quad \sinh \alpha = \frac{2 f_2 f_5 \sqrt{(f_4^2 - f_2^2)(f_4^2 - f_5^2)}}{f_4^2(f_2^2 - f_5^2)}. \tag{21}$$

Extra attenuation by staggering n sections:

$$\Delta\alpha = (n - 1)6 \text{ db}. \tag{22}$$

Note: To distinguish from sub-4 in VI type, substitute sub-4*a*, 4*b*, 4*c* in successive sections of V type. For sub-5, substitute sub-*a*, *b*, *c* (shortened from sub-5*a*, 5*b*, 5*c*).

quency, and one branch (C_4L_4) is resonant at the trap frequency (f_4).

It is noted that the V-type half-section is a combination of two simpler types (Shea, III_2 and IV_1 [1], [2]) with an intervening ideal transformer. There are some advantages in deriving the formulas for these parts separately and then combining them to form the V type, which was done for the present purpose. (The IV and VI types can likewise be subdivided, but this offers no advantage in the case of frequency patterns having ratio symmetry.)

The inverter form of whole section [Fig. 6(c)] contains two inverters and the shunt arms of two half-sections (B_5, $2B_{34}$, B_5). The attenuation diagram [Fig. 6(d)] shows the variations of the attenuation (2α of two half-sections) outside the pass band.

The first objective in the V type is the selection of a trap frequency (f_4) which will give equal attenuation at the two edges of the stop band (f_7, f_8). This is nearly the optimum for several like sections of V type between the VI-type half-sections, because the latter contribute much less attenuation in the stop band. There will be given some formulas for approximately computing the best trap frequency.

In several sections of V type, there is a set of unequal trap frequencies (f_{4a}, etc.) that will give greatest attenuation over the stop band. For the present case of three sections, such a set is indicated in Fig. 1. There has been derived for this development a simple and explicit procedure for approximately evaluating such a set of trap frequencies, but this procedure is beyond the present scope [16]. The principles are familiar.

There has been found a simple rule for the advantage to be gained by staggering the trap frequencies in this manner rather than repeating the same value. The minimum attenuation over the stop band is thereby increased by $(n-1)6$ db for n sections. Staggering the trap frequencies for three sections gives 12 db more attenuation.

The formulas to be given are based on the theoretical lumped constants of the ladder form, leading to the corresponding shunt arms of the inverter form. Some significant ratios are formulated, such as the susceptance ratio ($b = B/G$) and the resonance ratio (Q). In most cases, the formulas are given in such forms that the narrow-band approximations are simple and perhaps apparent. Ratios are expressed in terms of the cycle frequencies (f) but the radian frequencies (ω) may be substituted.

Table I gives the formulas for the VI type of Fig. 5. The specified value of the derivation constant ($m = 0.6$) gives a favorable pattern of image conductance at the

TABLE III
PRESENT DESIGN VALUES

Pass:	$f_1 = 3.05, f_2 = 3.55$ kmc.
Stop:	$f_7 = 3.70, f_8 = 4.00$.
(1)	$m = 0.6$
(2)	$f_c = 0.25$
(3)	$f_\infty = 0.3125$
(4)	$f_0 = 3.290$
(5)	$f_3 = 2.992, f_4 = 3.617$
(10)	$f_4 = 3.78$
(11)	$m_5 = 0.961$
(12)	$f_5 = 3.358$
(13)	$f_6 = 3.847$
Changing subscripts from 5 to a, b, c; and from 4 to $4a$, $4b$, $4c$:	
	$f_{4a} = 3.708$, $f_{4b} = 3.780$, $f_{4c} = 3.953$
(11)	$m_a = 0.951$, $m_b = 0.961$, $m_c = 0.973$,
(12)	$f_a = 3.378$, $f_b = 3.358$, $f_c = 3.337$
(9)	2 half-sections (VI), $2\alpha > 12.04$ db
(18)	$\alpha_7 = 1.75$ nap = 15.2 db
(19)	$\alpha_8 = 1.87$ nap = 16.2 db
Average:	$\alpha_{78} = 1.81$ nap = 15.7 db
(21)	min $\alpha = 1.77$ nap = 15.4 db
Total:	Stopband, min. attenuation:
	2 half-sections (VI) > 12.0 db
	6 half-sections (V) 94.2 db
	Stagger 3 sections 12 db
	>118.2 db

Note: See Fig. 7 for pattern of all frequencies.

termination whose midshunt arm includes the pair of trap resonators (f_3, f_4). Over the middle 0.8 of a narrow pass band, the image conductance departs from its mid-band value (G) by less than -0 and $+0.04$ of this value.

The formulas are simplified by starting with the low-pass analog and converting to the band-pass frequency scale with ratio symmetry.

Outside the trap frequencies, the image attenuation approaches but always exceeds the limiting value given by (9), which is 6 db per half-section. Therefore each of the end half-sections may be relied on for this much attenuation.

Table II gives the formulas for the V type of Fig. 6. The derivation of the V type involves a constant (m_5) which is slightly less than unity; it is expressed in a form to bring out its small difference from unity.

One problem in computation is the interrelation of the formulas for f_4 (10) and f_5 or m_5 (11, 12). The value of f_4 need be evaluated only approximately, because it is required only for optimizing the stop band attenuation and not for validity of the filter design. For this approximation, it is here sufficient to substitute f_0 for f_5 in (10) for computing f_4. As mentioned above, the staggering of f_4 in several sections is not formulated here although it is employed in the example to be described [16].

At the junction of two different half-sections in a common shunt arm, their susceptance ratios are merely added to get the composite value.

In each shunt arm, it is sufficient to specify the one or two trap frequencies and the susceptance ratios at the two cutoff frequencies. All lumped constants are then determined. This specification is considered to be the

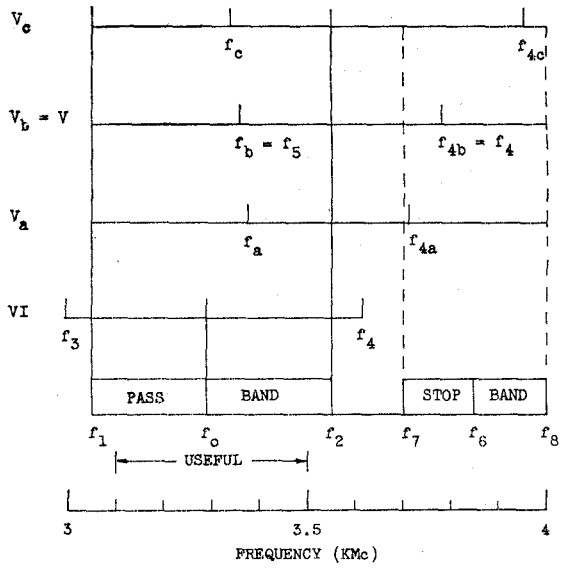

Fig. 7—Diagram of design frequencies.

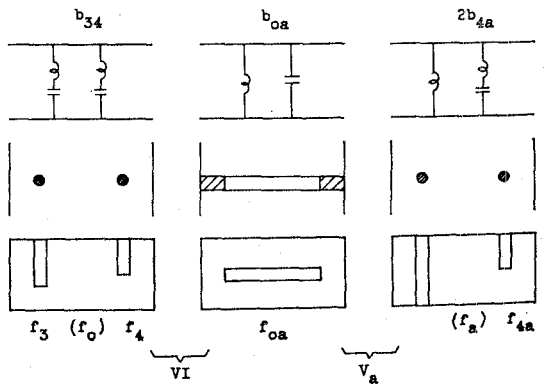

Fig. 8—Iris shunt arms in waveguide.

best basis for testing the simulation in a waveguide iris, because the trap frequencies are most easily measured and the susceptance is most critical near cutoff.

Table III gives the critical frequencies and attenuation computed for the present design. Fig. 7 is a diagram of these frequencies. The susceptance ratios are easily computed from the critical frequencies, to complete the specifications for the shunt arms.

SPECIFYING AND TESTING DISTRIBUTED ARMS

An iris in a waveguide is a distributed circuit complex that can be used to simulate a set of lumped constants, not exactly but to a close approximation. The approximation is best if the specifications are based on the most critical properties, and on those that can be tested most accurately. Naturally, any test must be based on a valid definition of the property to be simulated.

Fig. 8 shows the types of shunt arms that are to be simulated, and the iris structures to be used for this purpose. These are based on familiar principles. Each iris is resonant (zero susceptance) at a frequency in the pass band (f_0, f_{0a}, f_a). Two types have antiresonance (infinite susceptance) provided by posts resonant at the frequen-

cies noted. In general, all parts of one iris are interdependent. (The interaction between successive irises is ignored in computation but may require a small correction by experiment.)

For defining the objective of each shunt arm or iris, reference is made to the composite filter, as shown in Fig. 4. In the ladder form, one arm is isolated by properly removing the two adjacent arms. A shunt arm is isolated by an open-circuit in each adjacent series arm. Carrying this reasoning over to the inverter form, one shunt arm is isolated by a short-circuit on each adjacent shunt arm; through the inverter, this appears to be an open-circuit, as required.

This viewpoint is powerful because it gives a definition which may be interpreted to include the imperfections of the inverters, to a first approximation. Each shunt arm may utilize the small susceptance of the quarter-wave section, that remains at frequencies differing from its design frequency (presumably midband). Therefore, the susceptance of the arm at each end includes that of one quarter-wave section, while the susceptance of each intermediate arm includes twice that amount.

Fig. 9 shows how this principle may be applied in measuring the susceptance of one shunt arm in a waveguide. There are different procedures for an end arm or an intermediate arm, to be described with reference to Fig. 9(a).

In the case of an end arm, its susceptance is measured with a fixed short-circuit $\frac{1}{4}$ wavelength behind, so its susceptance is included as part of the shunt arm.

In the case of an intermediate arm, it is not so simple, because one side must be left accessible for the measurement. Measurements of the susceptance are made with a fixed short-circuit, first at $\frac{1}{4}$ and then at $\frac{3}{4}$ wavelength behind. The average of these two is the desired susceptance, which includes twice the susceptance of a quarter-wave section. Fig. 9(b) shows how these tests would appear on the rim of the reflection chart.

Since the iris has some thickness, however small, there is some question as to where the reference plane is. It can be determined by applying some insight in any particular case, if that degree of precision is needed [18].

The trap frequencies are most easily measured by the deep minimum in a transmission test. This is substantially independent of generator, load, and adjacent quarter-wave lines. A susceptance test should place this point on a pole of the reflection chart, such as f_4 in Fig. 9(b). (This fact may be used to locate the proper reference plane [18].)

By these techniques, an iris may be adjusted by trial to simulate a computed shunt arm in a waveguide. The entire filter is assembled from the 9 irises adjusted according to these formulas and rules.

Low-Power Tests

The low-power performance comprises frequency characteristics without regard for pulse-power capability, so there is no appreciable difference between air and vacuum. (Presumably, there is a slight difference caused by mechanical deformation under differential pressure.) The dimensions of essential contours were specified on the basis of tests in air, then transferred to the final design for evacuation.

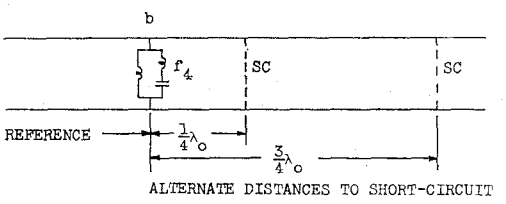

(a) Arrangement of iris in measuring line.

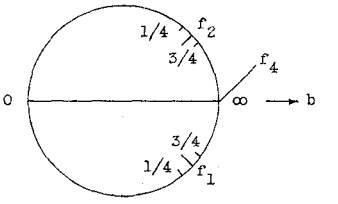

(b) Plot of observations on reflection chart.

Fig. 9—Test for susceptance of shunt arm in waveguide.

The tests to be presented were made on a single filter, between nonreflecting input and output waveguides, before installing the pressure windows. The performance in the pass band is plotted in Fig. 10 for the experimental model, all dimensions having been determined by separate tests of the irises. The performance is described in terms of reflection and attenuation.

The experimental model was found to have the pass band located about 1 per cent higher than intended, in frequency. Presumably this was caused by interaction between the irises, which were assumed independent, though separated only by a distance comparable with their height. By way of compensation, all dimensions were then specified 1 per cent larger than the model in order to center the actual pass band on the desired pass band. The curves in Fig. 10 are shifted, relative to the observed curves, 1 per cent lower in frequency, to show what would be expected after this change in dimensions.

In Fig. 10(a), the reflection is plotted in terms of standing-wave ratio (SWR) over the pass band. The upper curve (dotted line) was observed when first assembled after designing the irises individually, and represents the cumulative errors of the many dimensions and some approximations in the assumptions for equivalence to the lumped network. The lower curve (solid line) was observed after corrective elements (inductive posts) had been inserted in the quarter-wave section at each end. Before this correction, the reflection was within 6.5 db SWR over the useful band; afterward, it was within 4 db SWR.

In Fig. 10(b), the insertion loss is plotted from tests on the experimental model, after insertion of the corrective elements. It is the sum of two parts respectively caused by reflection and dissipation. The reflection loss

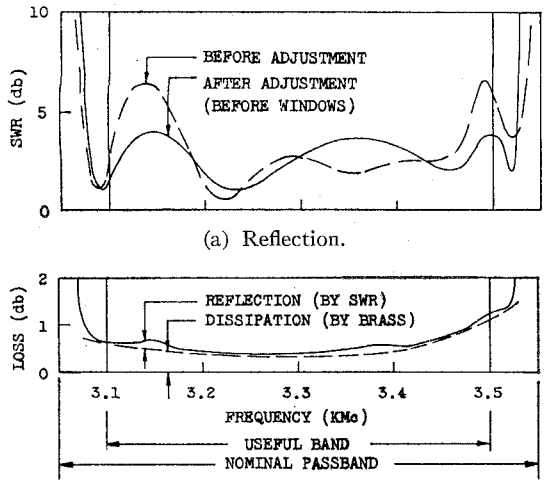

(a) Reflection.

(b) Attenuation.

Fig. 10—Reflection and attenuation in pass band.

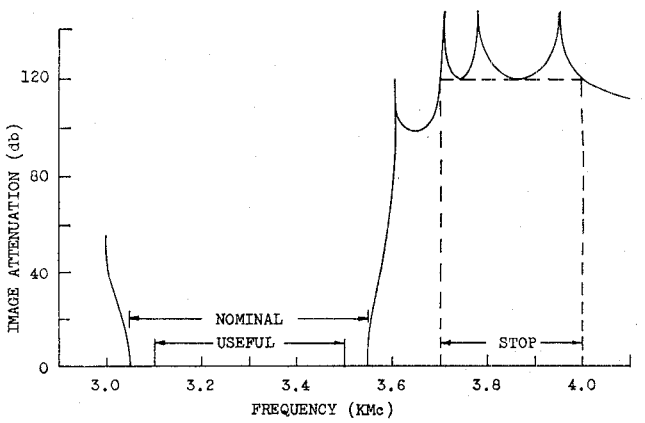

Fig. 11—Attenuation above pass band.

by about 0.2 db. The sum of these effects hold the dissipation loss. The reflection loss is related to the SWR plotted in Fig. 10(a). The remaining loss is caused by skin dissipation in the metal walls. The latter is proportional to phase slope over the pass band; it has a minimum value (about 0.3 db) at mid-band and increases at the edges of the useful band. The total insertion loss is within 1.2 db over the useful band, averaging about 0.6 db.

The properties of the experimental model are modified slightly by two differences in the final design, as follows:

	Experimental	*Final*
Metal walls	Brass	Copper
Pressure windows	Omitted	Included

The change from brass to copper reduces the skin dissipation by a factor of $\frac{1}{2}$. The addition of the glass windows for pressure sealing increases the dissipation loss within a lower limit, but leaves the average about the same. The windows slightly increase the reflection. The result is reflection within 6 db SWR and total insertion loss within 1.0 db over the useful band, averaging about 0.7 db.

In Fig. 11 is plotted the attenuation above the pass-band, computed on an image basis. It is over 120 db in the specified stop band. Tests of the experimental model over the stop band have verified that the attenuation exceeds 70 db, the limit of the equipment used. Interpretation of this information requires consideration of the modes in the waveguide.

As a general rule, when operating between input and output circuits of matched pure resistance, a lumped network provides an amount of insertion loss greater than the image attenuation. This rule would apply to the present case if we could consider only the propagating mode in the waveguide and ignore the higher modes. In the reduced size of waveguide chosen for the filter structure, the higher modes are propagated only above 4.3 kmc, which is well above the specified stop band. However, there remains some doubt whether the higher modes are negligible in the stop band. Another factor, probably of less importance, is the distributed nature of the iris shunt arms, which are assumed to simulate closely the lumped equivalents. In view of these considerations, it is uncertain whether the actual attenuation is greater or less than the computed image attenuation.

The nonreflecting assembly converts the wave filter (which attenuates only by reflection) into a selective attenuator. The attenuation in the stop band is substantially the same as the insertion loss caused by a single filter between nonreflecting input and output waveguides.

In the pass band, the reflection from the assembly is that of the hybrid junctions plus the uncanceled difference of the reflections from the pair of filters (since they will not be exactly alike). The difference of the transmission through the pair of filters causes a slight loss in recombination, which is added to the dissipation loss.

The discussion of Figs. 10 and 11 indicates the low-power performance to be expected of this design, and the extent to which this performance has been verified by tests.

High-Power Considerations

The nonreflecting assembly is intended to carry one-megawatt pulses of about one microsecond duration with some safety factor for moderate reflection from the load (say 3 db SWR). This means that each filter should be able to carry pulses of 0.5 megawatt into the reflecting load or 0.7 megawatt into a matched load, with some margin.

As is usually the case in pulse transmission, the power limitation is imposed by voltage breakdown in the dielectric, not by heating. This amount of pulse power is easily handled by air in ordinary waveguide and accessories, but the insertion of the resonators in the present filter tends to cause much higher gradients.

Such resonance can be obtained in a spacious cavity, such as a half-wave section of guide, without excessive gradient. However, this kind of resonator presents several difficulties. For the present purpose, the principal fault would be the failure of attenuation at frequencies somewhat higher than the pass band, where most at-

tenuation is required. Other handicaps are the greater size and the greater difficulty of choosing and simulating a suitable lumped network.

It was desired to realize the required resonance in the most compact form that could be readily predicted and constructed. The so-called "wide-band" TR tubes had a background of theory and structural experience, including evacuation and pressure sealing, so it was decided to use the same principles and general arrangement for the present filter. This decision was based on the idea of complete evacuation to prevent voltage breakdown, so fairly small gaps would stand the voltage.

In accordance with the practice in TR tubes, the partition for the simple resonant iris was made of fairly thin sheet ($\frac{1}{16}$ inch) for ease of construction. This required a slot of width comparable with the thickness (minimum about $\frac{1}{16}$ inch). The resulting small gap and the open ends of the resonant posts experience the highest gradient.

The voltage across the slot exceeds 20 kv rms and the maximum gradient reaches about 20 kv/mm rms, which is about 10 times that of air. Comparable gradients are experienced in the magnetron for which the present filter is designed. However, it has been found difficult to maintain in a cold structure the degree of evacuation and surface purity required to withstand this gradient without some kind of discharge.

Some samples have been made which carried pulse power through a pair of filters into a matched load, up to about 1 megawatt, the maximum used in the tests. Further improvements are in progress, particularly in the techniques of evacuation.

Conclusion

For suppressing spurious transmission from a certain *S*-band radar, there has been designed a nonreflecting filter assembly in which the principal feature is the pair of wave filters built in waveguide and evacuated to carry high-power pulses.

Each of these wave filters is made of 25 reactors or their equivalent in 9 reactance arms suitable for waveguide shunt arms. These involve 5 trap frequencies outside the pass band and some reasonance frequencies near midband. The image-parameter method of design, based on the wave-filter concept, has enabled all computations in explicit form. Among the features are *M*-derived terminations for impedance matching over the pass band, another type of section giving greatest attenuation above the pass band, and the staggering of the trap frequencies in several sections of this type for maximum attenuation over the stop band. This is the only method of design known to the writers that would yield comparable performance with a reasonable amount of effort.

The specifications for all reactance arms are presented in a form suitable for testing simulation in shunt arms made of irises in a waveguide. The recommended set of essential quantities includes only the trap frequencies and the susceptance ratios at the cutoff frequencies. The application of these formulas has yielded a practical design reasonably fulfilling the expectations based on the computations.

Acknowledgments

The writers wish to express their appreciation of the contributions and assistance of their associates, particularly I. Koffman, who performed most of the experimental work.

Bibliography

[1] T. E. Shea, "Transmission Networks and Wave Filters," D. Van Nostrand Co., Inc., New York, N. Y.; 1929. (Band-pass filters, pp. 315–318.)
[2] F. E. Terman, "Radio Engineers' Handbook," McGraw-Hill Book Co., Inc., New York, N. Y.; 1943. (Band-pass filters, pp. 230–231.)
[3] W. D. Lewis and L. C. Tillotson, "A non-reflecting branching filter for microwaves," *Bell. Sys. Tech. J.*, vol. 27, pp. 83–95; January, 1948. (Branching filter using hybrid junctions and quarter-wave path difference for band selection without causing reflection in input and output lines.)
[4] H. A. Wheeler, "Transmission lines and equivalent networks," *Wheeler Monographs*, vol. 1, no. 1; April, 1948. (Concept of inverter, references.)
[5] C. G. Montgomery, R. H. Dicke, and E. M. Purcell, "Principles of Microwave Circuits," *M.I.T. Rad. Lab. Ser.*, McGraw-Hill Book Co., Inc., New York, N. Y., vol. 8; 1948. (Resonant irises in waveguide, hybrid junctions, directional couplers.)
[6] A. W. Lawson and R. M. Fano, "The Design of Microwave Filters," M.I.T. Rad. Lab. Ser., McGraw-Hill Book Co., Inc., New York, N. Y., vol. 9, ch. 10, pp. 613–716; 1948. (Includes resonant irises spaced $\frac{1}{4}$ wavelength in waveguide, many references.)
[7] W. C. Caldwell, "Bandpass TR Tubes," M.I.T. Rad. Lab. Ser., McGraw-Hill Book Co., Inc., New York, N. Y., vol. 14, ch. 3, pp. 67–114; 1948. (Filters made of resonant irises spaced $\frac{1}{4}$ wavelength in waveguide, pressure windows, references.)
[8] C. W. Zabel, "Balanced Duplexers," M.I.T. Rad. Lab. Ser., McGraw-Hill Book Co., Inc., New York, N. Y., vol. 14, ch. 8, pp. 350–375; 1948. (Nonreflecting filter, properties of hybrid junctions.)
[9] H. A. Wheeler, "Generalized transformer concepts for feedback amplifiers and filter networks," *Wheeler Monographs*, vol. 1, no. 5; August, 1948. (Inverter concept between shunt arms, references.)
[10] W. W. Mumford, "Maximally-flat filters in waveguide," *Bell Sys. Tech. J.*, vol. 27, pp. 684–713; October, 1948. (Concept of inverter and shunt arms; references.)
[11] N. Marcuvitz, "Waveguide Handbook," M.I.T. Rad. Lab. Ser., McGraw-Hill Book Co., Inc., New York, N. Y., vol. 10; 1951. (Simulation of lumped circuits in waveguide structures.)
[12] H. J. Riblet, "The short-slot hybrid junction," PROC. IRE, vol. 40, pp. 180–184; February, 1952. (Properties of 3-db side-wall directional coupler, application to nonreflecting filter used as balanced duplexer, many references.)
[13] E. Hadge, "Compact top-wall hybrid junction," IRE TRANS. ON MICROWAVE THEORY AND TECHNIQUES, vol. MTT-1, pp. 29–30; March, 1953. (Pair of parallel slots in common wide face of parallel waveguides.)
[14] H. Heins, "Radar duplexer uses dual TR tubes," *Electronics*, vol. 27, pp. 149–151; August, 1954. (Nonreflecting filters, simple explanation.)
[15] C. W. Jones, "Broad-band balanced duplexers," IRE TRANS. ON MICROWAVE THEORY AND TECHNIQUES, vol. MTT-5, pp. 4–12; January, 1957. (Nonreflecting filter, side-wall and top-wall short-slot 3-db directional couplers as hybrid junctions.)
[16] H. A. Wheeler, "Image-Parameter Design of *S*-Band Waveguide Filter," Wheeler Labs., Great Neck, N. Y., Rep. 765; November 15, 1957. (The present topic, complete design formulas.)
[17] H. L. Bachman, "A Waveguide Filter for Suppressing the Spurious Transmission of a High-Power *S*-Band Radar," Wheeler Labs., Great Neck, N. Y., Rep. 764; 1958. (In preparation.) (Main report on this project, list of other reports, pp. 765–769.)
[18] H. L. Bachman, "Specifying and testing distributed elements in *S*-band waveguide filter," Wheeler Labs., Great Neck, N. Y., Rep. 766; April 16, 1958.
[19] R. D. Campbell, "Radar interference to microwave communication services," *AIEE Trans.*, Paper No. 58-817, preprinted and presented before AIEE; June, 1958. (The operational situation requiring the *S*-band filter described in present paper.)